A Mechanistic Study of the Ring Opening Reaction of Singlet Oxirane

Yukio Yamaguchi,† Henry F. Schaefer III,*,† and Ian L. Alberts‡

Contribution from the Center for Computational Quantum Chemistry, University of Georgia, Athens, Georgia 30602, and the Department of Chemistry, University of Edinburgh, Edinburgh EH9 3JJ, Scotland

Received September 30, 1992

Abstract: The C–C ring opening reaction of the oxirane molecule on the singlet potential energy surface has been investigated within the context of *ab initio* electronic structure theory. Self-consistent-field (SCF), two-configuration SCF (TCSCF), and configuration interaction with single and double excitations (CISD) levels of theory are employed in conjunction with two basis sets, double-ζ plus polarization (DZP) and triple-ζ plus double polarization (TZ2P). For the SCF and TCSCF methods, the TZ2P basis set supplemented with higher angular momentum functions, TZ(2df,-2pd), is also used. Ten stationary points are located on the singlet reaction surface and unambiguously characterized by analyzing the energy second derivatives (Hessian). Three minima are located on the surface corresponding to the closed-shell ring structure (as reactant) and two closed-shell open structures (as products) of C_2 and C_s symmetry. These minima are shown to be connected via four genuine transition states along the corresponding reaction coordinates. Planar open oxirane with C_{2v} symmetry (edge-to-edge, E-E isomer) is characterized as neither a minimum nor a transition state but as a higher order stationary point with Hessian index 2. The electrocyclic ring opening of the C–C bond in oxirane is shown to occur preferably through a conrotatory double methylene rotation pathway leading to the C_2 open structure with an activation energy of 52.0 kcal/mol with the zero-point vibrational energy (ZPVE) correction. No genuine transition state for the "forbidden" disrotatory mechanism is located within the constraint of C_s symmetry; instead the C_s stationary point exhibits two imaginary vibrational frequencies. This C_s stationary point lies 11.8 kcal/mol above the true C_2 symmetry transition state. The interconversion of the C_2 and C_s open minima appears to occur quite easily with a small activation energy. The asynchronous ring opening pathway and the single methylene rotation process (leading to net one-center epimerization) are predicted to have activation energies that are 7.5 and 7.7 kcal/mol (with the ZPVE correction), respectively, greater than the barrier for conrotatory ring opening. It is proposed that the energetic competition between the conrotatory, asynchronous, and single methylene rotation processes influences the stereochemistry of oxirane cycloaddition reactions. Reaction mechanisms are also suggested for the thermal geometrical isomerizations (epimerizations) of oxiranes.

1. Introduction

Oxirane derivatives have long been used as key intermediates in the synthesis of many organic compounds.[1] In solution, oxiranes are known to be susceptible to attack by both electrophilic and nucleophilic reagents. In addition, oxiranes can undergo unimolecular reactions that are thermally or photochemically induced, yielding ring opening or fragmented species. The unimolecular reactivity and structures of oxiranes OC_2R_4, and isoelectronic trimethylenes C_3R_6 and aziridines NC_2R_4, has formed an active area of chemical research both experimentally[2-19] and theoretically.[20-38]

Oxirane ring opening reactions lead to the formation of intermediates which are detectable via their 1,3-dipolar cycloaddition reactions with unsaturated systems.[4,7-10,25-27] These intermediates either close back to the ring form[5-11,25-27] (thus, the geometrical isomerization of oxiranes passes through the open intermediate) or partake in fragmentations yielding a range of species including carbonyl compounds and carbenes.[7,11,23,25-27] Oxirane ring opening may occur via C–C or C–O bond cleavage, and for oxirane derivatives the nature of the substituents often determines the preferred route. Alkyl substituents favor C–O rupture in both photochemically and thermally induced reactions,

† University of Georgia.
‡ University of Edinburgh.

(1) For a review, see: March, J. *Advanced Organic Chemistry: Reactions, Mechanisms and Structures*, 4th ed.; McGraw-Hill: New York; 1992.
(2) (a) Ullman, E. F.; Milks, J. E. *J. Am. Chem. Soc.* **1962**, *84*, 1315. (b) Ullman, E. F.; Milks, J. E. *J. Am. Chem. Soc.* **1964**, *86*, 3814.
(3) Huisgen, R.; Scheer, W.; Huber, H. *J. Am. Chem. Soc.* **1967**, *89*, 1753.
(4) (a) Linn, W. J.; Benson, R. E. *J. Am. Chem. Soc.* **1965**, *87*, 3657. (b) Linn, W. J. *J. Am. Chem. Soc.* **1965**, *87*, 3665.
(5) MacDonald, H. H. J.; Crawford, R. J. *Can. J. Chem.* **1972**, *50*, 428.
(6) Do-Minh, T.; Trozzolo, A. M.; Griffin, G. W. *J. Am. Chem. Soc.* **1970**, *92*, 1402.
(7) Griffin, G. W. *Angew. Chem., Int. Ed. Engl.* **1971**, *10*, 537.
(8) (a) Hamberger, H.; Huisgen, R. *J. Chem. Soc., Chem. Commun.* **1971**, 1190. (b) Dahmen, A.; Hamberger, H.; Huisgen, R.; Markowski, V. *J. Chem. Soc., Chem. Commun.* **1971**, 1192. (c) Markowski, V.; Huisgen, R. *J. Chem. Soc., Chem. Commun.* **1977**, 439. (d) Huisgen, R.; Markowski, V. *J. Chem. Soc., Chem. Commun.* **1977**, 440.
(9) Huisgen, R. *Angew. Chem., Int. Ed. Engl.* **1977**, *16*, 572.
(10) Wong, J. P. K.; Fahmi, A. A.; Griffin, G. W.; Bhacca, N. S. *Tetrahedron* **1981**, *37*, 3345.
(11) Békhazi, M.; Warkentin, J. *J. Am. Chem. Soc.* **1983**, *105*, 1289.
(12) Schwab, J. M.; Ho, C.-K. *J. Chem. Soc., Chem. Commun.* **1986**, 872.
(13) Freedman, T. B.; Paterlini, M. G.; Lee, N.-S.; Nafie, L. A.; Schwab, J. M.; Ray, T. *J. Am. Chem. Soc.* **1987**, *109*, 4727.
(14) Freedman, T. B.; Spencer, K. M.; Ragunathan, N.; Nafie, L. A.; Moore, J. A.; Schwab, J. M. *Can. J. Chem.* **1991**, *69*, 1619.
(15) (a) Gill, H. S.; Langrebe, J. A. *J. Org. Chem.* **1983**, *48*, 1051. (b) Gisch, J. F.; Langrebe, J. A. *J. Org. Chem.* **1985**, *50*, 2050.
(16) Berson, J. A. *Annu. Rev. Phys. Chem.* **1977**, *28*, 111.
(17) Engel, P. S. *Chem. Rev.* **1980**, *80*, 99.
(18) Gajewski, J. J. *Hydrocarbon Thermal Isomerizations*; Academic Press: New York, 1981; pp 27–35.
(19) (a) Cianciosi, S. J.; Ragunathan, N.; Freedman, T. B.; Nafie, L. A.; Baldwin, J. E. *J. Am. Chem. Soc.* **1990**, *112*, 8204. (b) Cianciosi, S. J.; Ragunathan, N.; Freedman, T. B.; Nafie, L. A.; Lewis, D. K.; Glenar, D. A.; Baldwin, J. E. *J. Am. Chem. Soc.* **1991**, *113*, 1864.
(20) Schilling, B.; Snyder, J. P. *J. Am. Chem. Soc.* **1975**, *97*, 4422.
(21) (a) Hayes, E. F. *J. Chem. Phys.* **1969**, *51*, 4787. (b) Hayes, E. F.; Siu, A. K. Q. *J. Am. Chem. Soc.* **1971**, *93*, 2090.
(22) (a) Yamaguchi, K.; Fueno, T. *Chem. Phys. Lett.* **1973**, *22*, 471. (b) Yamaguchi, K. *Chem. Phys. Lett.* **1975**, *33*, 330.
(23) (a) Bigot, B.; Sevin, A.; Devaquet, A. *J. Am. Chem. Soc.* **1979**, *101*, 1095. (b) Bigot, B.; Sevin, A.; Devaquet, A. *J. Am. Chem. Soc.* **1979**, *101*, 1101.
(24) Caramella, P.; Gandour, R. W.; Hall, J. A.; Deville, C. G.; Houk, K. N. *J. Am. Chem. Soc.* **1977**, *99*, 385.

0002-7863/93/1515-5790$04.00/0

whereas aryl substituents favor C–C cleavage.[23] Pertaining to unsubstituted oxirane, the pathway to formation of the C–O opened structure does not pass over a barrier according to theoretical studies.[23] Thus, the C–O open form is likely to reclose spontaneously back to the more stable oxirane ring structure. Ring opening via C–C cleavage does pass over a barrier, and thus the C–C opened structure is more susceptible to chemical analysis.

The mechanistic features of electrocyclic ring opening reactions of three-membered rings have been the subject of a number of works. Woodward and Hoffmann postulated that the electrocyclic conversion of cyclopropyl anion to allyl anion should be thermally "allowed" for conrotatory motion of the terminal methylene groups and photochemically "allowed" for disrotatory motion.[39,40] Following orbital symmetry arguments, the C–C ring opening of the isoelectric heterocyclic system oxirane should proceed in an analogous manner. Several theoretical investigations have verified that unsubstituted oxirane should open thermally in a conrotatory fashion and photochemically in a disrotatory manner.[23,25–27]

The relative energies of the stationary points located along the various ring opening reaction pathways naturally determine the preferred ring opening route. Volatron et al., employing a multireference configuration interaction procedure in conjunction with the 4-31G basis set, found the conrotatory ring opening stationary point of unsubstituted oxirane to be 10.9 kcal/mol lower in energy than the stationary point corresponding to disrotation.[27] In a recent study, we predicted a barrier of 56.4 kcal/mol for oxirane conrotatory ring opening via C–C bond cleavage using the two-reference configuration interaction with single and double excitations (CISD) level of theory with the double-ζ plus polarization (DZP) basis set.[41] The planar open structure displayed two imaginary harmonic vibrational frequencies, $589i$ (a_2) and $505i$ cm^{-1} (b_1), and, therefore, does not correspond to a true intermediate (minimum) on the oxirane potential energy hypersurface.[41] A C_2 symmetry open structure was located by Feller et al.[29] and Tachibana et al.[30] and found to be more stable than the planar edge-to-edge (E–E) isomer by less than 1 kcal/mol at the 4-31G two-configuration self-consistent-field (TCSCF) level of theory. Geometrical and energetic predictions have also been reported for the edge-to-edge (E–F) and face-to-face (F–F) open oxirane structures.[23,25–27] However, these conformers including the C_2 symmetry structure were not unambiguously characterized as minima or saddle points in previous studies.

For substituted oxiranes (and aziridines) experimental studies generally confirm the predicted modes of electrocyclization for thermal and photolytic reactions.[3–10] However, cycloaddition reactions of certain substituted oxiranes, for example, α-cyano-*cis*-stilbene oxide, lead to higher than expected yields of the "forbidden" products.[8–10] Proposals to account for such results have included rotational isomerization in the E–E open structure intermediate and direct participation of the forbidden "disrotatory" pathway.[8–10,26,27] The possibility of alternative explanations prompted the current reinvestigation of the singlet oxirane potential energy surface.

We report a relatively complete characterization of ten stationary points on the singlet oxirane potential energy hypersurface, including predictions of geometrical structures, harmonic vibrational frequencies, and relative energies of minima and transition states, using high-level theoretical techniques that include electron correlation effects. Energy differences between the various ring opening pathways are obtained and rationalized in terms of the applicability of the Woodward–Hoffmann rules for oxirane. These predictions are compared with the corresponding results for the second row analogue thiirane, SC_2H_4, reported previously.[41] The current theoretical results allow us to propose a suitable alternative explanation for the higher than expected yields of the "forbidden" product in cycloaddition reactions involving sterically hindered oxiranes. We also propose reaction mechanisms for geometrical isomerizations of oxirane molecules, including both one- and two-center epimerization processes.

2. Electronic Structure Considerations

Ten stationary points were located on the singlet oxirane potential energy surface in the present study. In order to appropriately describe the electronic structures of these isomers the minimum level of theory required is the two-configuration SCF (TCSCF) wave function, since ring opening reaction involves the C–C bond breaking. The electronic structure for the reactant, the closed shell ring $^1A_1$ state of oxirane, may be described by a single-configuration SCF wave function

$$[\text{core}](3a_1)^2(2b_2)^2(4a_1)^2(1b_1)^2(5a_1)^2(3b_2)^2(1a_2)^2(6a_1)^2(2b_1)^2 \quad (1)$$

For the purpose of direct comparisons with other structures a second configuration may be incorporated into the wave function for the ring isomer

$$[\text{core}](3a_1)^2(2b_2)^2(4a_1)^2(1b_1)^2(5a_1)^2(3b_2)^2(1a_2)^2(2b_1)^2(4b_2)^2 \quad (2)$$

resulting from the $(6a_1)^2 \rightarrow (4b_2)^2$ [$(\sigma_b)^2 \rightarrow (\sigma^*)^2$] double excitation. Two-configuration SCF (TCSCF) wave functions, involving simultaneous optimization of the coefficients of configurations (1) and (2) as well as the molecular orbital (MO) expansion coefficients, are suitable for this purpose.

For the "final" product of the ring opening reaction (according to Woodward–Hoffmann[39,40]), the closed shell planar $^1A_1$ edge-to-edge (E–E) isomer, two configurations are required and the TCSCF wave function may be expressed by[21–23,25–30]

$$[\text{core}](3a_1)^2(2b_2)^2(4a_1)^2(5a_1)^2(3b_2)^2(1b_1)^2(4b_2)^2(6a_1)^2(1a_2)^2 \quad (3)$$

and

$$[\text{core}](3a_1)^2(2b_2)^2(4a_1)^2(5a_1)^2(3b_2)^2(1b_1)^2(4b_2)^2(6a_1)^2(2b_1)^2 \quad (4)$$

The second configuration results from the $(1a_2)^2 \rightarrow (2b_1)^2$ [$(\pi_n)^2 \rightarrow (\pi^*)^2$] double excitation. In Figure 1 important high-lying occupied and low-lying unoccupied MOs of the reactant and "final" product involved in the C–C ring opening reaction are

(25) Houk, K. N.; Rondan, N. G.; Santiago, C.; Gallo, C. J.; Gandour, R. W.; Griffin, G. W. *J. Am. Chem. Soc.* **1980**, *102*, 1504.
(26) Jean, Y.; Volatron, F. *Chem. Phys. Lett.* **1981**, *83*, 91.
(27) (a) Volatron, F.; Anh, N. T.; Jean, Y. *J. Am. Chem. Soc.* **1983**, *105*, 2359. (b) Volatron, F. *Can. J. Chem.* **1984**, *62*, 1502.
(28) (a) Hiberty, P. C.; Leforestier, C. *J. Am. Chem. Soc.* **1978**, *100*, 2012. (b) Hiberty, P. C.; Ohanessian, G. *J. Am. Chem. Soc.* **1982**, *104*, 66.
(29) Feller, D.; Davidson, E. R.; Borden, W. T. *J. Am. Chem. Soc.* **1984**, *106*, 2513.
(30) Tachibana, A.; Koizumi, M.; Okazaki, I.; Teramae, H.; Yamabe, T. *Theor. Chim. Acta* **1987**, *71*, 7.
(31) Horsley, J. A.; Jean, Y.; Moser, C.; Salem, L.; Stevens, R. M.; Wright, J. S. *J. Am. Chem. Soc.* **1972**, *94*, 279.
(32) Kato, S.; Morokuma, K. *Chem. Phys. Lett.* **1979**, *65*, 19.
(33) Doubleday, C.; McIver, J. W.; Page, M. *J. Am. Chem. Soc.* **1982**, *104*, 6533.
(34) Goldberg, A. H.; Dougherty, D. A. *J. Am. Chem. Soc.* **1983**, *105*, 284.
(35) Yamaguchi, Y.; Osamura, Y.; Schaefer, H. F. *J. Am. Chem. Soc.* **1983**, *105*, 7506.
(36) Yamaguchi, Y.; Schaefer, H. F. *J. Am. Chem. Soc.* **1984**, *106*, 5115.
(37) Yamaguchi, Y.; Schaefer, H. F.; Baldwin, J. E. *Chem. Phys. Lett.* **1991**, *185*, 143.
(38) Getty, S. J.; Davidson, E. R.; Borden, W. T. *J. Am. Chem. Soc.* **1992**, *114*, 2085.
(39) (a) Woodward, R. B.; Hoffmann, R. *J. Am. Chem. Soc.* **1965**, *87*, 395. (b) Hoffmann, R.; Woodward, R. B. *J. Am. Chem. Soc.* **1965**, *87*, 2046.
(40) Woodward, R. B.; Hoffmann, R. *Angew. Chem., Int. Ed. Engl.* **1969**, *8*, 781.
(41) Fowler, J. E.; Alberts, I. L.; Schaefer, H. F. *J. Am. Chem. Soc.* **1991**, *113*, 4768.

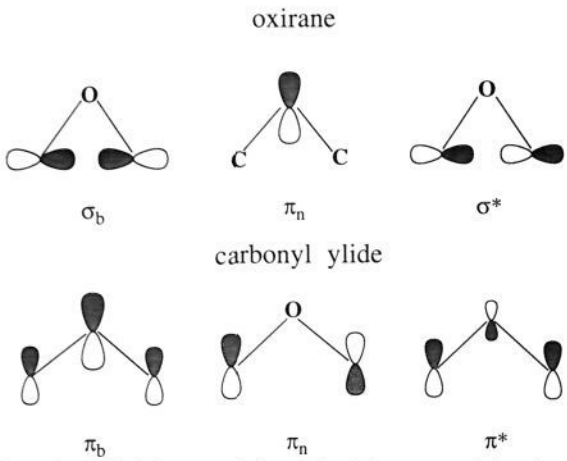

Figure 1. High-lying occupied and low-lying unoccupied molecular orbitals (MOs) of the reactant (oxirane) and "final" product (carbonyl ylide) involved in the C–C ring opening reaction.

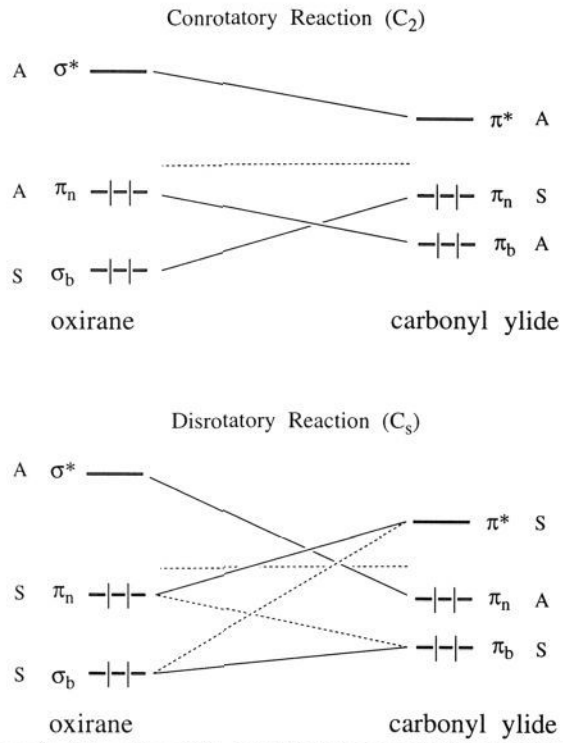

Figure 2. Schematic orbital correlation diagrams for the conrotatory and disrotatory ring opening of oxirane to carbonyl ylide.

schematically depicted. For other isomers the TCSCF wave functions may be constructed by carefully selecting the bonding and antibonding orbitals of the C–C bond. In Figure 2 orbital correlation diagrams for the conrotatory and disrotatory reactions have been displayed. The disrotory process involves a highest occupied MO (HOMO)–lowest unoccupied MO (LUMO) crossing which is characteristic of a Woodward–Hoffmann symmetry "forbidden" process. Conversely, the conrotatory process, with no HOMO-LUMO crossing, is referred to as Woodward–Hoffmann "allowed".

3. Theoretical Procedures

Three basis sets, labeled DZP, TZ2P, and TZ(2df,2pd), were employed in this study. The double-ζ plus polarization (DZP) basis set was the standard Huzinaga–Dunning double-ζ set of contracted Gaussian functions,[42,43] designated (9s5p/4s2p) for C, O and (4s/2s) for H, augmented with a single set of d-like polarization functions for C, O and p functions for H with exponents $\alpha_d(C) = 0.75$, $\alpha_d(O) = 0.85$, and $\alpha_p(H) = 0.75$. The basis set of triple-ζ plus double-polarization (TZ2P) quality involves the Huzinaga–Dunning[42,43] triple-ζ set of contracted Gaussian functions, designated (9s5p/5s3p) for C, O and (4s/3s) for H, augmented with two sets of polarization functions for each atom with orbital exponents $\alpha_d(C) = 1.50, 0.375$, $\alpha_d(O) = 1.70, 0.425$, and $\alpha_p(H) = 1.50, 0.375$. In these basis sets the hydrogen s functions have been scaled by the standard factor of 1.2. The TZ(2df,2pd) basis set was constructed by supplementing the TZ2P basis set with one set of f-like functions for the heavy atom with orbital exponents $\alpha_f(C) = 0.80$, $\alpha_f(O) = 1.40$ and one set of d-like functions for the hydrogen atom with orbital exponent $\alpha_d(H) = 1.0$. Complete sets of six Cartesian d-like functions and ten f-like functions were used throughout. The largest basis set, consisting of 168 contracted Gaussian functions, was used only for the SCF and TCSCF wave functions.

All the structures considered on the singlet oxirane potential energy surface have been completely optimized within the given symmetry constraints employing either restricted Hartree–Fock (RHF) SCF[44,45] or TCSCF[32,46] analytic first derivative techniques. Residual Cartesian and internal coordinate gradients are in all cases less than 10^{-6} atomic units. Quadratic force constants were evaluated using analytic SCF[47,48] or TCSCF[35,49] second derivative procedures. All stationary points were characterized via the resulting harmonic vibrational frequencies.

Configuration interaction with single and double excitation (CISD) energies with the DZP and TZ2P basis sets were determined at the SCF and TCSCF optimized geometries. In the CISD procedure only the valence electrons were explicitly correlated, thus the three lowest occupied (C 1s; O 1s-like) MOs were held doubly occupied (frozen cores) and the three highest lying virtual (C 1s*; O 1s*-like) orbitals were deleted (frozen virtuals). Otherwise, all single and double excitations from the SCF or TCSCF reference configuration were included (CISD). The DZP and TZ2P CISD wave functions with the TCSCF reference for the oxirane ring isomer in C_{2v} symmetry involved 57 484 and 199 730 configurations and for the conrotatory transition state in C_2 symmetry 113 521 and 395 366 configurations, respectively. The DZP and TZ2P CISD wave functions with the open-shell singlet SCF reference for the E–F isomer in C_s symmetry contain 71 513 and 246 108 configurations, respectively, in the Hartree–Fock interacting space.[50,51] These CISD wave functions were determined via the shape driven graphical unitary group approach.[52] The contributions from unlinked cluster quadruple excitations to the CISD energies were estimated using the Davidson correction,[53] or its two-reference analogue, and results incorporating this refinement are denoted CISD+Q.

4. Results

The optimized geometries of the ten stationary points located in this study are presented in Figures 3–7. In Table I the total energies and the TCSCF CI coefficients and in Table II the Hessian indices (numbers of imaginary frequencies) and the imaginary frequencies of these isomers are displayed. The complete harmonic vibrational frequencies of the ten stationary points, as well as the total energies, the CI coefficients, dipole moments, and the zero-point vibrational energies (ZPVE's), are provided as supplementary material. The TZ2P TCSCF values will be discussed in the text in order to compare directly with the corresponding thiirane results.

Geometries and Vibrational Analyses. (a) Ring (Cyclic, C_{2v}) Isomer. The electronic configuration of cyclic oxirane given by

(42) Huzinaga, S. *J. Chem. Phys.* **1965**, *42*, 1293.
(43) Dunning, T. H. *J. Chem. Phys.* **1970**, *53*, 2823.
(44) Pulay, P. *Modern Theoretical Chemistry*; Schaefer, H. F., Ed.; Plenum: New York, 1977; Vol. 4, p 53.
(45) Dupuis, M.; King, H. F. *J. Chem. Phys.* **1978**, *68*, 3998.
(46) Goddard, J. D.; Handy, N. C.; Schaefer, H. F. *J. Chem. Phys.* **1979**, *71*, 1525.
(47) Saxe, P.; Yamaguchi, Y.; Schaefer, H. F. *J. Chem. Phys.* **1982**, *77*, 5647.
(48) (a) Osamura, Y.; Yamaguchi, Y.; Saxe, P.; Vincent, M. A.; Gaw, J. F.; Schaefer, H. F. *Chem. Phys.* **1982**, *72*, 131. (b) Osamura, Y.; Yamaguchi, Y.; Saxe, P.; Fox, D. J.; Vincent, M. A.; Schaefer, H. F. *J. Mol. Struct.* **1983**, *103*, 183.
(49) (a) Yamaguchi, Y.; Osamura, Y.; Fitzgerald, G.; Schaefer, H. F. *J. Chem. Phys.* **1983**, *78*, 1607. (b) Duran, M.; Yamaguchi, Y.; Remington, R. B.; Schaefer, H. F. *Chem. Phys.* **1988**, *122*, 201.
(50) Bunge, A. *J. Chem. Phys.* **1970**, *53*, 20.
(51) Bender, C. F.; Schaefer, H. F. *J. Chem. Phys.* **1971**, *55*, 4798.
(52) Saxe, P.; Fox, D. J.; Schaefer, H. F.; Handy, N. C. *J. Chem. Phys.* **1982**, *77*, 5584.
(53) Langhoff, S. R.; Davidson, E. R. *Int. J. Quantum Chem.* **1974**, *8*, 61.

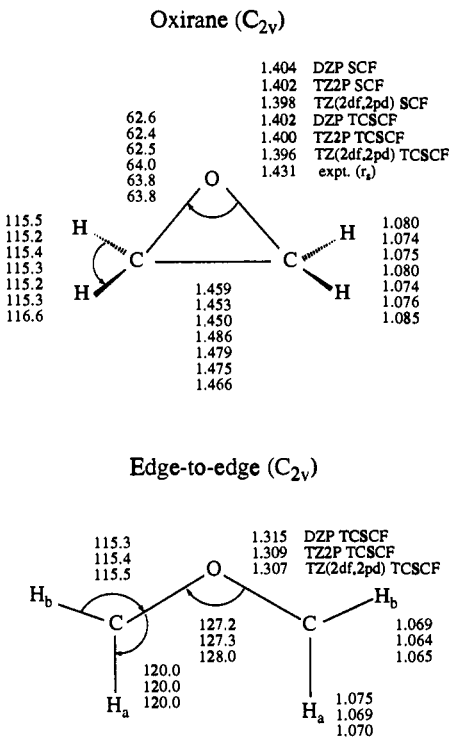

Figure 3. (a) Predicted equilibrium geometry for oxirane (C_{2v}). (b) Predicted geometry for the E–E stationary point (C_{2v}, Hessian index 2). Bond lengths are in angstroms and bond angles in degrees. Experimental structural parameters are from ref 54.

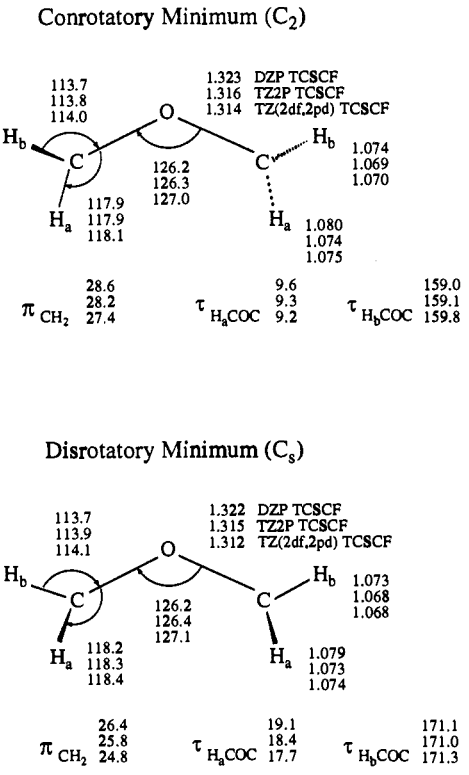

Figure 4. (a) Predicted geometry for the conrotatory minimum (C_2) of oxirane. (b) Predicted geometry for the disrotatory minimum (C_s). Bond lengths are in angstroms and bond angles in degrees. The extent of the methylene group pyramidalization, π_{CH_2}, is measured as the angle formed between the C–O bond and the plane of the CH_2 group.

eqs 1 and 2 implies single bonding within the COC ring. This is exemplified by the C–O and C–C bond distances of 1.400 and 1.479 Å, respectively, at the TZ2P TCSCF level, which are typical single bond distances for cyclic compounds. In comparison with the thiirane ring TCSCF optimized geometry with a TZ2P basis

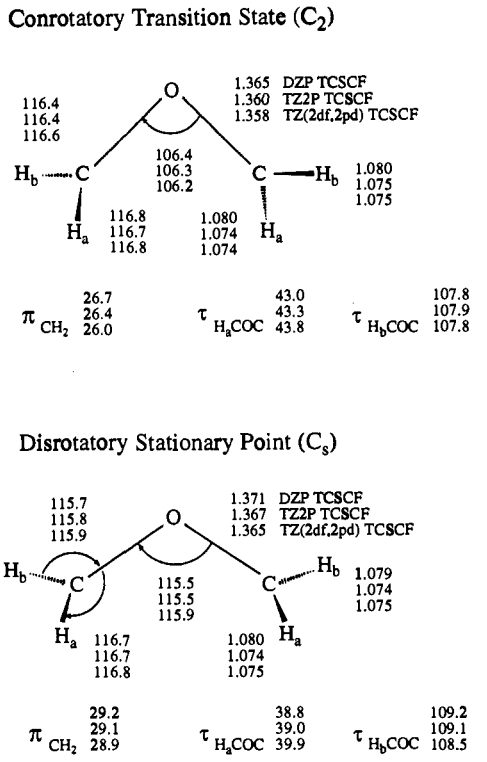

Figure 5. (a) Predicted geometry for the conrotatory transition state (C_2) of oxirane. (b) Predicted geometry for the disrotatory stationary point (C_s, Hessian index 2). Bond lengths are in angstroms and bond angles in degrees. The extent of the methylene group pyramidalization, π_{CH_2}, is measured as the angle formed between the C–O bond and the plane of the CH_2 group.

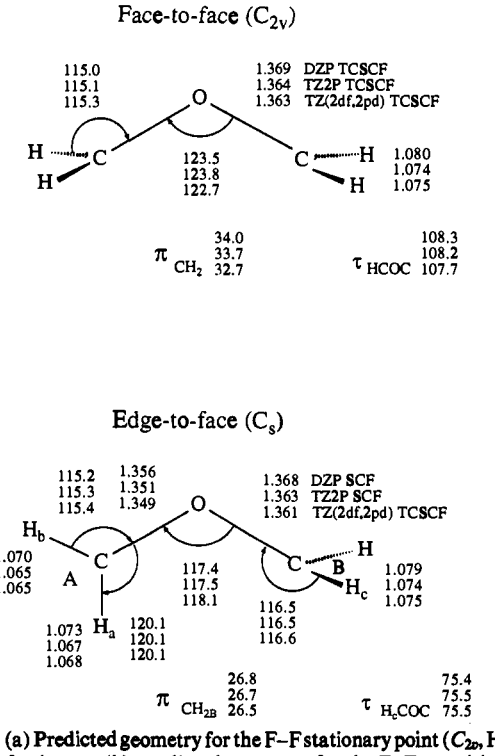

Figure 6. (a) Predicted geometry for the F–F stationary point (C_{2v}, Hessian index 3) of oxirane. (b) Predicted geometry for the E–F transition state (C_s). Bond lengths are in angstroms and bond angles in degrees. The extent of the methylene group pyramidalization, π_{CH_2}, is measured as the angle formed between the C–O bond and the plane of the CH_2 group.

set, the great disparity in C–O and C–S bond distances leads to very different ring angles, 63.8° (COC) in oxirane and 48.6° (CSC) in thiirane, and C–C distances, 1.479 Å in oxirane and 1.495 Å in thiirane. The predicted SCF and TCSCF structural

First C_1 Transition State

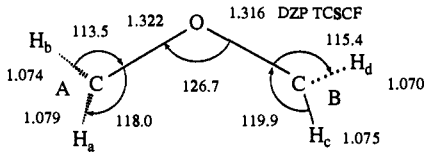

π CH_{2A} 27.9 τ H_aCOC 15.9 τ H_cCOC 8.0

π CH_{2B} 5.0 τ H_bCOC 166.2 τ H_dCOC 177.2

Second C_1 Transition State

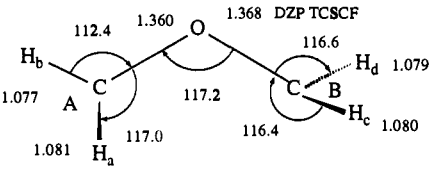

π CH_{2A} 34.6 τ H_aCOC 31.5 τ H_cCOC 77.7

π CH_{2B} 27.1 τ H_bCOC 174.4 τ H_dCOC 72.8

Figure 7. (a) Predicted geometry for the C_2–C_s interconversion transition state (C_1) for oxirane. (b) Predicted geometry for the asynchronous ring opening transition state (C_1). Bond lengths are in angstroms and bond angles in degrees. The extent of the methylene group pyramidalization, π_{CH_2}, is measured as the angle formed between the C–O bond and the plane of the CH_2 group.

parameters of the oxirane ring are reasonably close to the experimental values.[54]

The ring isomer is characterized as a minimum on the potential energy surface, since all harmonic vibrational frequencies with both SCF and TC-SCF methods are real. The two CO stretching frequencies, 1358 (symmetric) and 968 cm^{-1} (asymmetric) at the TZ2P TCSCF level of theory, are typical values for the cyclic C–O single bond.

(b) E–E (Planar, C_{2v}) Isomer. The electronic configuration of the planar $^1A_1$ E–E open isomer given by eqs 3 and 4 implies C–O multiple bonding in conjunction with a larger COC angle (no C–C bonding) relative to the ring structure. The C–O distance of 1.309 Å at the TZ2P TCSCF level of theory is significantly shorter than the single bond length of 1.400 Å in the ring isomer and is closer to typical C–O double bond distances. In comparison with the analogous thiirane structure, the COC bond angle of 127.3° at the TZ2P TCSCF level of theory is again larger than the CSC angle of 113.7° in open E–E thiirane at the equivalent level of theory, due to the significantly shorter C–O distance relative to C–S. The CI coefficients in the TZ2P TCSCF wave function for the oxirane E–E isomer, $C_1 = 0.910$ and $C_2 = -0.416$, clearly indicate the diradical character of this ylide molecule.[21-23,25-30]

Planar E–E oxirane displays two imaginary vibrational frequencies, 586*i* cm^{-1} (a_2) and 500*i* cm^{-1} (b_1) at the TZ2P TCSCF level of theory. These modes correspond to the conrotatory and disrotatory distortions of the methylene groups. Thus, this isomer is characterized as neither a minimum nor a transition state, but as a higher order saddle point with Hessian index 2. In contrast, for the planar E–E structure of thiirane, the TZ2P TCSCF optimized geometry is found to be a minimum with a small magnitude real a_2 torsional frequency of 60 cm^{-1}. This difference in behavior can be explained by the greater C–O π antibonding character in the TCSCF wave function for planar E–E oxirane (the coefficient of the second configuration has larger magnitude) relative to planar thiirane, leading to the preference for nonplanar structures. Applying the second order Jahn–Teller effect, the above behavior can also be explained by the mixing of the excited $^1A_2$ and $^1B_1$ electronic states with the ground $^1A_1$ state in conjunction with a_2 and b_1 symmetry molecular displacements, respectively.[30] For E–E oxirane, the mixing is sufficient to provide a stabilizing effect on nonplanar molecular distortions; however, our studies suggest that is not the case for E–E thiirane. The asymmetric CO stretch frequency, 1609 cm^{-1} at the TZ2P TCSCF level of theory, is larger for the E–E isomer relative to the corresponding value for the oxirane ring molecule. This blue-shift may be attributed to the shorter C–O bond length for the ylide.

(c) C_2 (Conrotatory) and C_s (Disrotatory) Minima. The optimized geometries of the conrotatory and disrotatory isomers are very similar and are also close to that of the planar E–E structure. The most noteworthy features are the longer C–O bond distances for the C_2 and C_s structures relative to the planar conformer due to reduction of orbital overlap in the π space. This destabilizing effect is balanced by pyramidalization of the terminal methylene groups with angles of 28.2° for the conrotatory isomer and 25.8° for the disrotatory structure. Here an extent of the pyramidalization is measured as the angle formed by the CO bond and the plane of the CH_2 group. The CI coefficients in the TZ2P TCSCF wave function are $C_1 = 0.900$ and $C_2 = -0.436$ for the C_2 structure, while they are $C_1 = 0.899$ and $C_2 = -0.438$ for the C_s structure. These CI coefficients are reasonably close to those for the E–E isomer mentioned above. C_2 and C_s minima were not located for thiirane with the TCSCF method.

Following the a_2 imaginary mode of the E–E isomer discussed above into C_2 symmetry leads to the location of the ^1A conrotatory structure. On the other hand, reoptimization in C_s symmetry along the b_1 imaginary mode of the E–E isomer yields the $^1A'$ disrotatory structure. For these two structures all harmonic vibrational frequencies are real, indicating that they are equilibrium geometries. The conrotatory and disrotatory vibrational modes are of sufficiently large magnitude to give rise to no ambiguity in this conclusion. The asymmetric CO stretching frequencies for C_2 and C_s minima, 1568 and 1574 cm^{-1}, respectively, at the TZ2P TCSCF level, have about the same magnitude as the corresponding value of 1609 cm^{-1} for the E–E isomer.

(d) C_2 (Conrotatory) Transition State and C_s (Disrotatory, Hessian Index 2) Stationary Point. These two stationary points display similar geometrical structures, the major difference being the COC bond angle, 106.3° (C_2) vs. 115.5° (C_s) at the TZ2P TCSCF level of theory. This can be explained by the considerably greater magnitude of the second configuration in the TZ2P TCSCF wave function leading to larger C–O and C–C antibonding character for the disrotatory stationary point, $C_1 = 0.730$ and $C_2 = -0.683$, relative to the conrotatory stationary point, $C_1 = 0.875$ and $C_2 = -0.485$. This argument also rationalizes the slightly longer C–O distance in the C_s stationary point. The angles of methylene rotation for the two stationary points are 43.3° (C_2) and 39.0° (C_s), close to halfway between the 90° for the ring structure and the 9.3° or 18.4° for the C_2 or C_s open equilibrium structures. The corresponding thiirane conrotatory and disrotatory stationary points show similar geometrical trends.[41] Taking into account the C–O distances and COC angles, it is evident that the stationary points for conrotatory and disrotatory ring opening are geometrically closer to the corresponding C_2 or C_s symmetry minima (product) than the ring isomer (reactant).

The conrotatory stationary point yields a single imaginary vibrational frequency of a symmetry, 378*i* cm^{-1} at the TZ2P

(54) Hirose, C. *Bull. Chem. Soc. Jpn.* **1974**, *47*, 1311.
(55) Dewar, M. J. S.; Kirschner, S. *J. Am. Chem. Soc.* **1974**, *96*, 5244.
(56) Yates, B. F.; Yamaguchi, Y.; Schaefer, H. F. *J. Chem. Phys.* **1990**, *93*, 8798.

Table I. Total Energies (in kcal/mol) and TCSCF CI Coefficients for the Singlet Oxirane System[a,b]

molecule	oxirane	E–E (C_{2v})	C_2 min.	C_s min.	C_2 t.s.	C_s s.p.	F–F (C_{2v})	E–F (C_s)	C_1 t.s. first	C_1 t.s. second
DZP (TC)SCF	–0.921 590	–0.853 086	–0.855 438	–0.854 424	–0.841 361	–0.828 102	–0.824 665	–0.830 260	–0.853 984	–0.832 825
C_1	0.994	0.908	0.898	0.897	0.872	0.729	0.747	1.000	0.902	0.713
C_2	–0.113	–0.419	–0.440	–0.443	–0.489	–0.684	–0.665	0.000	–0.431	–0.701
TZ2P (TC)SCF	–0.931 826	–0.864 220	–0.866 469	–0.865 466	–0.852 082	–0.838 665	–0.834 781	–0.840 700		
C_1	0.994	0.910	0.900	0.899	0.875	0.730	0.747	1.000		
C_2	–0.112	–0.416	–0.436	–0.438	–0.485	–0.683	–0.665	0.000		
TZ(2df,2pd) (TC)SCF	–0.939 635	–0.871 591	–0.873 606	–0.872 644	–0.858 369	–0.845 124	–0.841 429	–0.847 358		
C_1	0.994	0.911	0.901	0.901	0.876	0.731	0.735	1.000		
C_2	–0.111	–0.413	–0.433	–0.434	–0.483	–0.682	–0.678	0.000		
DZP CISD	–1.336 655	–1.265 795	–1.266 281	–1.265 512	–1.247 463	–1.229 993	–1.225 499	–1.234 039	–1.265 810	–1.235 636
TZ2P CISD	–1.400 666	–1.331 979	–1.331 761	–1.331 272	–1.312 278	–1.294 559	–1.289 999	–1.298 901		
DZP CISD+Q	–1.382 567	–1.312 006	–1.312 249	–1.311 519	–1.292 692	–1.274 276	–1.269 430	–1.278 606	–1.311 916	–1.280 099
TZ2P CIDS+Q	–1.453 456	–1.385 354	–1.384 781	–1.384 373	–1.364 490	–1.345 691	–1.340 832	–1.350 357		

[a] Add –152.000 000 hartrees to all energies. [b] CISD and CISD+Q energies are at the TCSCF optimized geometries.

Table II. Hessian Indices and Imaginary Frequencies (in cm^{-1}) for the Singlet Oxirane System[a,b]

molecule	Hessian index	imaginary freq	approx assign
oxirane	0		
E–E (C_{2v})	2	586*i* (a_2)	CH_2 wag
		500*i* (b_1)	CH_2 wag
C_2 minimum	0		
C_s minimum	0		
C_2 transition state	1	378*i* (a)	CH_2 twist
C_s stationary point	2	586*i* (a′)	CH_2 twist
		218*i* (a″)	CH_2 twist
F–F (C_{2v})	3	310*i* (a_1)	COC deform
		292*i* (a_2)	CH_2 twist
		355*i* (b_1)	CH_2 twist
E–F (C_s)	1	721*i* (a″)	CH_{2A} wag
first C_1 transition state	1	520*i* (a)	CH_{2B} wag
second C_1 transition state	1	527*i* (a)	CH_{2B} twist

[a] Frequencies are determined at the TZ2P TCSCF level of theory. [b] Frequencies for the C_1 symmetry isomers are determined at the DZP TCSCF level of theory.

TCSCF level of theory. Not surprisingly, the reaction coordinate for this imaginary frequency corresponds to conrotation of the methylene groups strongly coupled with a contribution from COC angle deformation and leads to the C_2 equilibrium open structure. The C_2 symmetry stationary point is, therefore, a genuine transition state for the conrotatory electrocyclic ring opening of oxirane via C–C cleavage.

On the other hand, the disrotatory stationary point displays two imaginary vibrational frequencies with the TZ2P TCSCF method of 586*i* cm^{-1} (a′) and 218*i* cm^{-1} (a″). The magnitudes of the imaginary frequencies do not change appreciably with increase in the basis set from DZP to TZ(2df,2pd); thus, there is no ambiguity as to the "occurrence" of these imaginary vibrations. The normal coordinate for the a′ mode corresponds to the expected disrotatory methylene rotation and leads to the C_s equilibrium open structure. The normal coordinate for the a″ mode involves conrotatory methylene rotation and releases (lowers) the C_s symmetry of the stationary point leading to a lower order stationary point in C_1 symmetry. These results bear a close resemblance to the analogous thiirane ring opening reaction pathways.[41] The asymmetric CO stretching frequencies 1310 cm^{-1} for the C_2 transition tate (t.s.) and 1332 cm^{-1} for the C_s (with Hessian index 2, hereafter abbreviated as H2) stationary point (at the TZ2P TCSCF level of theory) are significantly smaller than the corresponding values for the E–E isomer, C_2 and C_s minima, reflecting the longer CO bond lengths.

(e) F–F (C_{2v}) Isomer. A further possible structure for open oxirane is the face-to-face (F–F) conformation. The diradical nature of this $^1A_1$ state is emphasized by the CI coefficients in the TZ2P TCSCF wave function, $C_1 = 0.747$ and $C_2 = -0.665$. For this isomer the C–O bond length, 1.364 Å, is close to that for the C_2 (t.s.) and C_s (H2) stationary points, while the COC bond angle, 123.8°, is close to that for the C_2 and C_s minima. The pyramidalization of the terminal methylene groups with angles of 33.7° for the F–F isomer is larger than that for the C_2 and C_s minima.

The harmonic vibrational analysis shows the $^1A_1$ F–F structure to have three imaginary vibrational frequencies at the TZ2P TCSCF level of theory. These correspond to COC angle deformation, 310*i* cm^{-1} (a_1), and conrotatory, 292*i* cm^{-1} (a_2), and disrotatory, 355*i* cm^{-1} (b_1), rotation of the terminal methylene groups. The a_1 mode leads to the ring structure, while the a_2 and b_1 modes lead to the conrotatory C_2 (t.s.) and disrotatory C_s (H2) stationary points, respectively. The asymmetric CO stretching frequency of 1379 cm^{-1} with the same method is close to those for the C_2 (t.s.) and C_s (H2) transition species.

(f) E–F (C_s) Isomer. The structure of the E–F isomer involves a pyramidalization angle of 26.7° for the nonplanar methylene group and C–O distances of 1.351 and 1.363 Å at the TZ2P SCF level of teory. The carbon of the in-plane methylene group is involved in π bonding to the oxygen, whereas the rotation and pyramidalization of the out-of-plane methylene group relieves C–O π bonding on this side of the molecule leading to a longer C–O bond distance. The C–O distances and the COC bond angle, 117.5°, appear to be closer to those for the C_2 (t.s.) and C_s (H2) stationary points than the corresponding minima.

The open-shell $^1A''$ E–F structure yields one imaginary vibrational frequency, 721*i* cm^{-1}, of a″ symmetry at the TZ2P SCF level of theory, corresponding to a wagging motion of the planar CH_2 group. Following this mode in either direction leads to the ring structure. The E–F structure, thus, corresponds to a genuine transition state for the rotation of a single methylene group leading to net one-center stereomutation (epimerization) of the oxirane ring. In the absence of such a vibrational analysis, several workers incorrectly suggested that the E–F structure corresponds to a transition state for rotational isomerization in open oxirane (i.e. E–E → E–F → E–E).[25-27] The asymmetric CO stretching frequency of 1388 cm^{-1} (at the TZ2P TCSCF level of theory) is close to those for the C_2 (t.s.) and C_s (H2) stationary points.

(g) First C_1 Transition State. The optimized geometry of the first C_1 symmetry stationary point (Figure 7a) shows one methylene group pyramidalized and the other relatively close to coplanarity with the COC unit. The C–O distances, 1.322 and 1.316 Å, COC angle, 126.7°, and pyramidalization angle for the nonplanar methylene group, 27.9°, are very similar to the

Table III. Relative Energies (in kcal/mol) for the Singlet Oxirane System[a,b]

molecule	oxirane	E–E (C_{2v})	C_2 min.	C_s min.	C_2 t.s.	C_s s.p.	F–F (C_{2v})	E–F (C_s)	C_1 t.s. first	C_1 t.s. second
DZP (TC)SCF	0.0	31.9	30.4	31.0	39.2	47.5	49.7	46.2	31.3	44.6
	(0.0)	(43.0)	(41.5)	(42.1)	(50.3)	(58.7)	(60.8)	(57.3)	(42.4)	(55.7)
	[0.0]	[–]	[38.7]	[38.9]	[46.5]	[–]	[–]	[52.3]	[38.6]	[51.5]
TZ2P (TC)SCF	0.0	31.2	29.8	30.4	38.8	47.2	49.7	46.0		
	(0.0)	(42.4)	(41.0)	(41.6)	(50.0)	(58.5)	(60.9)	(57.2)	(–)	(–)
	[0.0]	[–]	[38.2]	[38.5]	[46.2]	[–]	[–]	[52.2]	[–]	[–]
TZ(2df,2pd) (TC)SCF	0.0	31.5	30.3	30.9	39.8	48.1	50.5	46.7	–	–
	(0.0)	(42.7)	(41.4)	(42.0)	(51.0)	(59.3)	(61.6)	(57.9)	(–)	(–)
	[0.0]	[–]	[38.6]	[38.9]	[47.2]	[–]	[–]	[52.9]	[–]	[–]
DZP CISD	0.0	41.5	41.2	41.6	53.0	63.9	66.7	61.4	41.5	60.4
	(0.0)	(44.5)	(44.2)	(44.6)	(56.0)	(66.9)	(69.8)	(64.4)	(44.5)	(63.4)
	[0.0]	[–]	[41.4]	[41.4]	[52.2]	[–]	[–]	[59.4]	[40.7]	[59.2]
TZ2P CISD	0.0	39.9	40.0	40.3	52.3	63.4	66.2	60.7	–	–
	(0.0)	(43.1)	(43.2)	(43.5)	(55.5)	(66.6)	(69.4)	(63.9)	(–)	(–)
	[0.0]	[–]	[40.4]	[40.4]	[51.7]	[–]	[–]	[58.9]	[–]	[–]
DZP CISD+Q	0.0	43.0	42.8	43.3	55.1	66.6	69.7	63.9	43.0	63.0
	(0.0)	(44.3)	(44.1)	(44.6)	(56.4)	(68.0)	(71.0)	(65.2)	(44.3)	(64.3)
	[0.0]	[–]	[41.3]	[41.4]	[52.6]	[–]	[–]	[60.2]	[40.5]	[60.1]
TZ2P CISD+Q	0.0	41.2	41.6	41.8	54.3	66.1	69.2	63.2	–	–
	(0.0)	(42.7)	(43.1)	(43.3)	(55.8)	(67.6)	(70.7)	(64.7)	(–)	(–)
	[0.0]	[–]	[40.3]	[40.2]	[52.0]	[–]	[–]	[59.7]	[–]	[–]

[a] The values (in parentheses) are relative to the one-configuration (or two-configuration) reference. [b] The values in brackets are relative to the two-configuration reference with the zero-point vibrational energy (ZPVE) correction.

corresponding values in the C_2 and C_s minima. The CI coefficients for this transition state are $C_1 = 0.902$ and $C_2 = -0.431$, which are also close to those for the C_2 and C_s minima.

The first C_1 symmetry stationary point shows one imaginary vibrational frequency, $520i$ cm^{-1}, at the DZP TCSCF level of theory. The normal coordinate for this mode involves a wagging motion of one of the methylene groups (the group almost coplanar with the COC atoms). Following this mode in one direction leads to the C_2 symmetry minimum and in the other direction to the C_s symmetry minimum. This C_1 structure, thus, corresponds to a genuine transition state for the interconversion of the C_2 and C_s equilibrium open structures. The asymmetric CO stretching frequency of 1619 cm^{-1} with the DZP TCSCF method is close to those for the corresponding mode of the E–E stationary point and the C_2 and C_s minima.

(h) **Second C_1 Transition State.** The optimized geometry of the second C_1 symmetry stationary point (Figure 7b) shows significant pyramidalization and rotation of the methylene groups with respect to the plane defined by the COC atoms. The two C–O distances, 1.360 and 1.368 Å, are close to the C–O distance for the C_s (H2) stationary point and that in the E–F structure involving the pyramidalized methylene group. The C_s (H2) stationary point, E–F structure, and this C_1 stationary point also display similar COC angles, 115.5°, 117.5°, and 117.2°, respectively. The strong diradical character of this structure is shown clearly by the CI coefficients in the DZP TCSCF wave function, $C_1 = 0.713$ and $C_2 = -0.701$. As a whole this C_1 structure displays a general geometrical feature common to both the C_s (H2) stationary point and the E–F isomer.

The second C_1 symmetry stationary point yields one imaginary vibrational frequency, $527i$ cm^{-1}, at the DZP TCSCF level of theory. The normal coordinate for this mode involves a twisting motion of the nonplanar methylene group, moderately coupling with a twisting motion of the near planar methylene group. Following this mode in one direction leads to the structure formally implied to be the disrotatory product and in the other direction to the ring structure. This C_1 symmetry structure probably corresponds to the transition state for asynchronous ring opening discussed by Voltron et al.[27] and suggested previously by Dewar and Kirshner in a theoretical investigation of "forbidden" electrocyclic reactions.[55] The asymmetric CO stretching frequency of 1396 cm^{-1} is close to the corresponding values for the C_2 (t.s.), C_s (H2), and E–F (t.s.) stationary points.

Relative Energies. The energy differences between the various stationary points located on the singlet oxirane potential energy surface are presented in Table III. The values for each structure are relative to the one-configuration and two-configuration (in parentheses) reference energies for the ring structure. The values in brackets are relative to the two-configuration reference with the zero-point vibrational energy (ZPVE) correction.

The oxirane ring structure is the well-known global minimum on the singlet potential energy hypersurface. The secondary minima, the C_2 and C_s open structures, are 40.3 and 40.2 kcal/mol (both with the ZPVE correction), respectively, higher in energy at the TZ2P CISD+Q level of theory. These two open minima are very close energetically, separated by less than 0.6 kcal/mol, at all theoretical levels considered in this research. In comparison, the thiirane open structure – ring energy difference is 34.7 kcal/mol (with the ZPVE correction) at the corresponding TZ2P CISD+Q level of theory.[41]

The oxirane and thiirane ring opening reactions display very similar mechanistic and energetic behavior. The conrotatory ring opening pathway via the C_2 symmetry transition state requires an activation energy of 52.0 kcal/mol (with the ZPE correction) (TZ2P CISD+Q) for oxirane, compared to the corresponding thiirane behavior of 51.3 kcal/mol (with the ZPVE correction) at the equivalent level of theory. The C_s symmetry disrotatory stationary points are 11.8 (oxirane) and 15.6 kcal/mol (thiirane) higher energetically than the conrotatory transition state, in accordance with the Woodward–Hoffmann rules[39,40] for each system.

The barrier heights for the conrotatory ring closure reactions of oxirane and thiirane are 11.7 (with the ZPVE correction; relative to the oxirane C_2 minimum) and 16.6 kcal/mol (with the ZPVE correction; relative to planar open thiirane), respectively, large enough to suggest possible laboratory isolation of the unsubstituted open structures.

The single methylene rotation mechanism, via the $^1A''$ E–F transition state, has an activation energy of 59.7 kcal/mol (with the ZPVE correction) using the TZ2P CISD+Q method. The conrotatory ring opening pathway is, thus, favored by 7.7 kcal/mol (with the ZPVE correction) relative to the single methylene rotation pathway. The interconversion between the C_2 and C_s equilibrium open minima, via the first C_1 symmetry transition state, is found to have a classical activation energy of only 0.9 kcal/mol at the DZP TCSCF level of theory. There appears to be no barrier for this interconversion at the CISD and CISD+Q levels of theory. Thus, the two open forms interconvert quite

readily. The asychronous ring opening transition state (the second C_1 symmetry transition state) lies 60.1 kcal/mol (with the ZPVE correction) above the ring isomer and is comparable energetically to the E–F transition state at the DZP CISD+Q level of theory.

The final stationary point located on the singlet oxirane potential energy surface, the $^1A_1$ F–F isomer, which shows three imaginary vibrational frequencies (Hessian index 3), is 70.7 kcal/mol above the ring isomer at the TZ2P CISD+Q level of theory.

Our best values for energy differences in this study are given by the TZ2P CISD+Q method (one reference or two references where appropriate) since this procedure includes the major electron correlation effects and yields accurate energetic predictions (see, for example, ref 56). From an examination of Table III, the relative energies appear close to convergence with respect to theoretical level and basis set size. However, basis set enhancement at the correlated levels, for example augmenting the TZ2P basis set with f functions, may change the energy differences by about 1.0 kcal/mol, and inclusion of higher order excitations from the SCF (or TCSCF) reference wave functions, e.g., CISDTQ, may lead to further changes of the order of 1.0 kcal/mol. The zero-point vibrational energy (ZPVE) may also introduce errors of about 0.5 kcal/mol. Thus the error bar in our energetic predictions is about 2.5 kcal/mol.

5. Discussion

The relative energies and character of the various stationary points located on the singlet oxirane potential energy surface allow a depiction of the reaction modes for geometrical isomerization of (isotopically) substituted oxiranes.

The minimum energy pathway for thermal two-center (optical) epimerization of oxiranes follows closely the scheme discussed previously for cyclopropane.[37,38] The reaction pathway initially involves conrotatory ring opening of the oxirane molecule through the conrotatory transition state to the C_2 symmetry open minimum. Beyond this point a branching or bifurcation point is encountered from which two degenerate pathways diverge. These pathways essentially correspond to a rotation and flattening of one of the two methylene groups leading to equivalent C_1 symmetry transition states. From this pair of stationary points the methylene groups invert, culminating in equivalent C_s symmetry open minima. The degenerate pathways then each involve motion of the second methylene group until another pair of equivalent C_1 symmetry transition states is reached. The second methylene group is then inverted and the degenerate pathways converge and intersect giving another C_2 symmetry open minimum. Passage over another conrotatory transition state yields the net two-center epimerized oxirane ring. The conrotatory transition state corresponds to the highest point on the route to double epimerization. From an examination of the kinetics of the thermal racemization of *trans*- and *cis*-2-phenyl-3-*p*-tolyloxirane, Crawford and MacDonald[5] suggested a mechanism for the process involving thermal conrotatory ring opening/closure in agreement with the initial and final steps of the two-center epimerization discussed above. The difference in our mechanism is the releasing of C_2 symmetry constraint to avoid passing over the E–E stationary point with Hessian index 2.

An alternative pathway for thermal epimerization of (isotopically) substituted oxiranes may involve the asynchronous route. The highest point along the asynchronous pathway lies 7.5 kcal/mol (with the ZPVE correction) above the conrotatory transition state; thus, an asynchronous ring opening could be followed by closure in either a conrotatory (leading to one-center epimerization) or asynchronous (leading to two-center epimerization) fashion.

Thermal one-center epimerization can also occur via passage over the E–F transition state. Rotation and pyramidalization of the methylene groups of the oxirane molecule lead to the E–F (C_s symmetry) transition state and ring closure from this point yields the net one-center epimerized structure. Since the activation energy for the single methylene rotation pathway is 7.7 kcal/mol (with the ZPVE correction) above the barrier for conrotatory ring opening, a molecule with sufficient energy to undergo one-center epimerization can also undergo two-center epimerization. *Cis–trans* isomerization reactions of suitably substituted oxiranes are expected to occur via the single methylene rotation pathway as well as the asynchronous route. These processes do not involve rotational isomerization of the open structure as has been suggested by other workers,[5,8–10,25–27] since the reaction coordinate for the imaginary frequency of the E–F transition state does not pass through the E–E structure. The one- and two-center epimerizations of cyclopropane molecules are believed to follow similar routes,[37,38] the main exception being the possible involvement of the formal disrotation process since a genuine disrotatory transition state for cyclopropane ring opening is located in C_s symmetry and found to be energetically very close to the conrotatory and E–F transition states.

In the presence of a dipolarophile under the appropriate reaction conditions, oxirane molecules can undergo cycloaddition reactions. The reaction pathway involves initial C–C cleavage to the open form, which is then trapped in a cycloadduct before reclosing. The stereochemistry of the cycloaddition product is dependent on the oxirane ring opening reaction mechanism. For unsubstituted oxirane, the important feature is that the conrotatory ring opening transition state is respectively 7.5 and 7.7 kcal/mol (with the ZPVE correction) lower in energy than the transition states for the asynchronous ring opening and the single methylene rotation. In the absence of steric constraints, cycloaddition reactions of oxiranes, therefore, should involve initial conrotatory ring opening leading to high stereoselectivity of the "allowed" cycloadduct. This prediction has been confirmed in a number of experimental studies.[8–10]

The loss of stereospecificity observed in sterically hindered species is the result of a loss of stereochemical purity in the ring opened structure.[8–10,26,27] From an analysis of our theoretical results, we propose that this loss of stereospecificity is due to the asynchronous ring opening procedure and the single methylene rotation process (one-center epimerization) becoming energetically competitive with the conrotatory ring opening mechanisms as a result of steric effects. Cycloaddition reactions of oxiranes in the presence of such steric effects, therefore, follow three distinct pathways (though not necessarily to equal extents): (i) conrotatory ring opening giving the "allowed" open structure, (ii) asynchronous ring opening giving the "forbidden" open structure (formally implied by direct C_s symmetry disrotation), and (iii) single methylene rotation to the one-center epimerized oxirane followed by conrotatory ring opening giving the "forbidden" open structure. When trapped with the dipolarophile these pathways lead to the formation of both "allowed" and "forbidden" cycloadducts and consequently a loss of stereoselectivity.

Cycloaddition reactions of α-cyano-*trans*-stilbene oxide and α-cyano-*cis*-stilbene oxide serve to illustrate the above proposal.[8,9,27] For the *trans* isomer, conrotatory ring opening (leading to the *exo,exo* structure) does not suffer from significant steric hindrance. The conrotatory barrier is expected to be sufficiently below the asynchronous ring opening and the single methylene rotation barriers to ensure the high stereoselectivity of the "allowed" product in cycloaddition reactions.

Conversely, a loss of stereoselectivity is encounted in cycloaddition reactions involving the *cis* isomer. Conrotatory ring opening of the *cis* form (path 1) leads to a sterically hindered C_2 open (*exo,endo*) structure ("allowed") with a bulky phenyl group in an *endo* position. The asychronous ring opening process directly produces a thermodynamically more stable, less sterically hindered, "forbidden" open (*exo,exo*) structure (path 2) with bulky phenyl groups in the more spacious *exo* positions. One-center epimerization leading to the *trans* oxide followed by conrotatory

ring opening of the *trans* form (path 3) also gives the "forbidden" open (*exo,exo*) structure. For the *cis* oxide, according to the Hammond postulate,[57] the transition state for conrotatory ring opening (highest point on path 1) will be destabilized relative to the transition states for asynchronous ring opening (highest point on path 2) and single methylene rotation (highest point on path 3) and the three routes are, thus, expected to be energetically competitive. Hence, cycloaddition reactions of the *cis* oxide involve participation of paths 1 through 3 leading to a mixture of "allowed" and "forbidden" open stereoisomers. This consequently results in a loss of stereoselectivity in the cycloaddition products. The extent of steric hindrance and the magnitude of the energy difference between the activation barriers for the conrotatory ring opening, asynchronous ring opening, and single methylene rotation pathways, therefore, directly affect the stereochemistry of the cycloaddition reactions of many substituted oxirane molecules.

Experimental work performed by Huisgen and co-workers verifies the above analysis.[8,9] In the case of α-cyano-*trans*-stilbene oxide, the conrotatory ring opening reaction barrier is experimentally estimated to be 3 kcal/mol *lower* in energy than the single methylene rotation barrier. The observed cycloaddition reactions of the *trans* isomer exhibit no loss of stereoselectivity with cycloaddition products, consistent with conrotatory ring opening. For α-cyano-*cis*-stilbene oxide, the conrotatory ring opening barrier is experimentally estimated to be 2 kcal/mol *above* the single methylene rotation barrier. Although Huisgen assumed rotational isomerization of the open structure (contrary to our theoretical results) and his estimated relative energies, derived from kinetic studies, could not distinguish between the asynchronous and the single-methylene rotation pathways, a loss of steroselectivity is, thus, predicted and has been observed in cycloaddition reactions involving the *cis* isomer (42% "allowed" and 53% "forbidden" cycloadducts observed).

6. Conclusions

The most stable structure on the singlet oxirane potential energy surface is the ring isomer which is found to lie below the C_2 and C_s open secondary minima by 40.3 and 40.2 kcal/mol (with the ZPVE correction), respectively. There is a very small barrier for interconversion between these two open minima. The ring opening reaction of unsubstituted oxirane via C–C cleavage is predicted to follow a mechanism involving conrotatory motion of the terminal methylene groups with an activation energy of 52.0 kcal/mol, the top of the barrier corresponding to a genuine transition state. There is no true transition state for the strictly disrotatory mechanism within the C_s symmetry point group and, in accordance with the "forbidden" nature of this pathway, the disrotatory stationary point is found to be 11.8 kcal/mol higher in energy than the conrotatory transition state.

However, an asynchronous pathway in C_1 symmetry was located with an activation barrier that is 7.5 kcal/mol above that for the conrotation process. The single methylene rotation pathway, leading to a net one-center epimerization, passes through the E–F transition state and shows an activation energy that is 7.7 kcal/mol above the barrier for conrotatory ring opening.

The minimum energy pathway on the potential energy surface for the two-center epimerization of, for instance, deuterated oxiranes involves initial conrotatory motion of the methylene groups leading to a C_2 open minimum, followed by a release of the C_2 symmetry to avoid passing through the C_{2v} E–E open structure with Hessian index 2. The symmetry lowering involves inversion of one methylene group and passage over a C_1 symmetry transition state to give a C_s symmetry minimum. This is followed by inversion of the second methylene group via another C_1 transition state yielding another C_2 open minimum, with subsequent conrotatory reclosure to the doubly epimerized ring.

Oxiranes in the absence of significant steric hindrance are expected to undergo highly stereospecific cycloaddition reactions. Steric effects, however, may affect the stereochemistry of the products of oxirange cycloaddition reactions. On the basis of our theoretical findings, we conclude that a loss of stereochemical purity of the open structure and, thus, of the subsequent cycloaddition product is likely to originate from energetic competition between conrotatory ring opening, asynchronous ring opening, and single-center epimerization, rather than direct C_s symmetry disrotatory ring opening or rotational isomerization of the open structure as proposed in earlier studies.[8-10,26,27]

Acknowledgment. We thank Professor John E. Baldwin at Syracuse University for many helpful discussions on this work. This research was supported by the U.S. Department of Energy, Office of Basic Energy Sciences, Division of Chemical Sciences, Fundamental Interactions Branch, Grant No. DE-FG09-87ER13811.

Supplementary Material Available: Tables giving theoretical predictions of the physical properties for the ten stationary points of oxirane (11 pages). Ordering information is given on any current masthead page.

(57) Hammond, G. S. *J. Am. Chem. Soc.* **1955**, *77*, 334.